c-axis transport and resistivity anisotropy of lightly to moderately doped $La_{2-x}Sr_xCuO_4$ single crystals: Implications on the charge transport mechanism

Seiki Komiya,* Yoichi Ando,† X. F. Sun, and A. N. Lavrov
Central Research Institute of Electric Power Industry, Komae, Tokyo 201-8511, Japan
(Received 20 January 2002; published 17 June 2002)

Both in-plane and out-of-plane resistivities (ρ_{ab} and ρ_c) are measured in high-quality $La_{2-x}Sr_xCuO_4$ single crystals in the lightly to moderately doped region $0.01 \leqslant x \leqslant 0.10$, and the resistivity anisotropy is determined. In all the samples studied, the anisotropy ratio ρ_c/ρ_{ab} quickly increases with decreasing temperature, although in nonsuperconducting samples the strong localization effect causes ρ_c/ρ_{ab} to decrease at low temperatures. Most notably, it is found that ρ_c/ρ_{ab} at moderate temperatures (100–300 K) is almost completely independent of doping in the nonsuperconducting regime ($0.01 \leqslant x \leqslant 0.05$); this indicates that the same charge confinement mechanism that renormalizes the *c*-axis hopping rate is at work down to $x=0.01$. It is discussed that this striking x independence of ρ_c/ρ_{ab} is consistent with the idea that holes form a self-organized network of hole-rich regions, which also explains the unusually metallic in-plane transport of the holes in the lightly doped region. Furthermore, the data for $x>0.05$ suggest that the emergence of the superconductivity is related to an increase in the *c*-axis coupling.

DOI: 10.1103/PhysRevB.65.214535 PACS number(s): 74.25.Fy, 74.25.Dw, 74.72.Dn, 74.20.Mn

I. INTRODUCTION

The mechanism of normal-state charge transport remains one of the central issues in the studies of the high-T_c cuprates, because it is intimately tied to the peculiarities of a strongly correlated electron system in which the high-T_c superconductivity is realized. The contrasting behavior between the in-plane resistivity ρ_{ab} and the *c*-axis resistivity ρ_c is arguably the most unusual property of the charge transport in cuprates (Ref. 1); namely, there is an intriguing coexistence of a metallic behavior in $\rho_{ab}(T)$ ($d\rho_{ab}/dT>0$) and an ''insulating'' (or semiconducting) behavior in $\rho_c(T)$ ($d\rho_c/dT<0$) in many cuprates,[2–4] and such an unusual nature of the anisotropic charge transport appears to offer a key to understanding the charge transport mechanism. In fact, a large amount of works have already concentrated on this issue.[5] Probably the most important feature in *c*-axis transport is that the magnitude of $\rho_c(T)$ is orders of magnitude larger than that expected from the band-structure estimate;[6] this indicates that there is some ''charge confinement'' mechanism[1] that renormalizes the *c*-axis hopping rate to a much smaller value. It has been argued that such ''confinement'' gives evidence of a non-Fermi-liquid nature of the cuprates,[1] and the persistence of the contrasting behavior between $\rho_{ab}(T)$ and $\rho_c(T)$ down to very low temperature[4] does indeed suggest that some unconventional mechanism is responsible for the charge confinement, since any Fermi-liquid-based mechanism that provides an apparent confinement at finite temperatures should saturate at low enough temperature.[7–9]

While it is likely that some unconventional mechanism (possibly a non-Fermi-liquid ground state) is fundamentally responsible for the confinement of charges into the CuO_2 planes (i.e., renormalization of the *c*-axis hopping rate), recent studies have shown[10–12] that a combination of the pseudogap and the **k** dependence of the *c*-axis matrix element[13] is largely responsible for the steeply insulating behavior of $\rho_c(T)$ observed, in particular, in $Bi_2Sr_2CaCu_2O_{8+\delta}$ (Bi-2212); namely, angle-resolved photoemission spectroscopy (ARPES) measurements of Bi-2212 have demonstrated[14] that the pseudogap causes a destruction of the Fermi surface starting from the $(0,\pm\pi)$ and $(\pm\pi,0)$ points, and the *c*-axis matrix-element effect[10,13] tends to amplify the contribution of the electrons on these gapped portions of the Fermi surface to the *c*-axis transport. As a result, the *c*-axis conductivity is quickly diminished upon opening of the pseudogap; the steep upturn in $\rho_c(T)$ observed in $YBa_2Cu_3O_{7-\delta}$ (YBCO),[3] Bi-2212,[15,16] and $Bi_2Sr_2CuO_{6+\delta}$ (Bi-2201) (Ref. 17) below the pseudogap temperature is considered to be due to this mechanism. On the other hand, it has been shown by ARPES measurements that the Fermi surface of the $La_{2-x}Sr_xCuO_4$ (LSCO) system appears to be quite different from that of Bi-2212 (the stripe fluctuations cause the Fermi surface to be one-dimensional- like[18,19]), and it is not likely that the pseudogap shows a similar development on the Fermi surface of the LSCO; therefore, it would be illuminating to examine the *c*-axis transport of LSCO, particularly in the underdoped region, and compare it with that of other cuprate systems.

In the past, *c*-axis transport in LSCO has already been rather well studied through various techniques, such as resistivity,[2,20–22] magnetoresistance,[23,24] microwaves,[25] and optics.[26,27] This is partly because large single crystals can be grown with the traveling-solvent floating-zone (TSFZ) technique for LSCO, and thus it is easy to obtain samples that are long enough along the *c* axis to allow reliable *c*-axis transport measurements. It has been demonstrated[2] that $\rho_c(T)$ in slightly underdoped samples ($0.10<x<0.16$) shows only a weak temperature dependence at moderate temperatures (100–300 K), particularly after correcting for the thermal expansion,[22] which is in contrast to the behaviors of $\rho_c(T)$ of Bi-2212 or Bi-2201,[15–17] where the pseudogap causes $\rho_c(T)$ to become steeply insulating. The magnetoresistance study by Hussey *et al.*[24] showed that the *c*-axis transport of LSCO

is incoherent, and that ρ_c is governed in a large part by the in-plane scattering rate. The low-temperature normal-state behavior of $\rho_c(T)$ in LSCO has been found to track the behavior of ρ_{ab}, namely, both $\rho_{ab}(T)$ and $\rho_c(T)$ for $0.08 \leqslant x \leqslant 0.15$ show a peculiar localizing behavior with the same temperature dependence of $\log(1/T)$ (Refs. 21 and 28); this seems to be in good accord with the magnetoresistance result of Hussey *et al.*,[24] which suggested that the strong in-plane scattering can cause the carriers to localize in both the *ab* and *c* directions.

However, all the *c*-axis transport studies that used TSFZ-grown single crystals have been limited to the region with $x \geqslant 0.06$; thus it is important to expand the region of x to smaller values, down to the lightly doped region, to establish a complete picture of the *c*-axis transport in LSCO. Since we recently succeeded in growing a series of high-quality single crystals of LSCO from $x=0.01$ to 0.17, and have measured their in-plane transport properties,[29] it is natural for us to study the *c*-axis transport using those high-quality single crystals. [There were studies of the transport properties of flux-grown $La_2CuO_{4+\delta}$ single crystals in the antiferromagnetic regime,[30,31] but the data were inconsistent with the present study (for ρ_c) and with Ref. 29 (for ρ_{ab}).] Studies of the *c*-axis transport in the lightly doped LSCO would be particularly useful for clarifying the mechanism of the *c*-axis transport, in view of the unusually metallic behavior of the in-plane mobility which suggests that the holes are likely to form a self-organized network of hole-rich regions where a band-like metallic transport occurs.[29] (Such a phase was theoretically predicted to be realized in correlated electron systems and was named ''electronic liquid crystal.''[32]) Also, recent ARPES measurements[19] provided information about the Fermi surfaces of lightly doped LSCO, which is useful in interpreting the transport data.

In this paper, we detail our technique to grow high-quality LSCO single crystals and present the *c*-axis transport data taken on the crystals with $x=0.01$–0.10. The corresponding $\rho_{ab}(T)$ data for the same compositions are also presented for the analysis of the resistivity anisotropy. It is found that the resistivity anisotropy ratio ρ_c/ρ_{ab} at moderate temperatures becomes almost independent of x in the lightly doped region; this is contrary to the common belief that the resistivity anisotropy should increase with decreasing doping and thus is a surprising result. We discuss that this striking x independence of ρ_c/ρ_{ab} is consistent with the idea that holes are segregated into a network of hole-rich regions, and that the *c*-axis transport is essentially an incoherent hopping between these self-organized networks, in which the strength of the ''confinement'' does not change with x.

II. EXPERIMENTAL DETAILS

A. Crystal growth and preparation

The series of $La_{2-x}Sr_xCuO_{4-\delta}$ single crystals ($0.01 \leqslant x \leqslant 0.10$) are grown by the TSFZ technique. Raw powders of La_2O_3, $SrCO_3$, and CuO (with purities of 99.9% or higher) are dried at 600 °C for 12 h prior to weighing, and then are weighed and mixed with a composition in which CuO is 2–3% richer than the nominal one; the additional CuO works as a binder of the polycrystalline feed-rod, and helps to avoid the occurrence of cracks in the rod, as well as avoiding penetration of the molten liquid into it, during the TSFZ operation. Also, since the vapor pressure of CuO during the growth is relatively high and thus the resulting crystals should have a smaller Cu content compared to the starting material, the excess CuO in the feed-rod compensates for the Cu loss and is necessary to obtain stoichiometric single crystals as the final product.

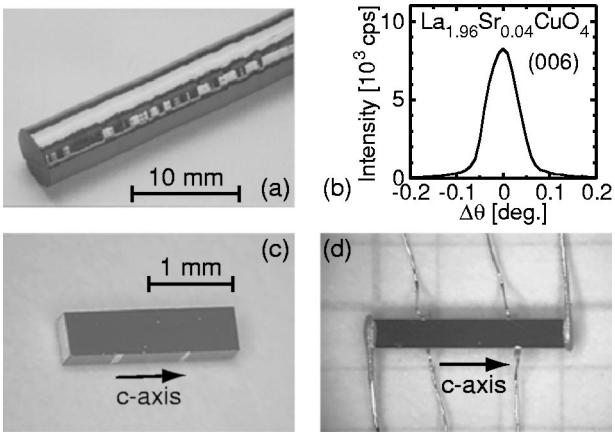

FIG. 1. (a) Photograph of a TSFZ-grown crystal with $x=0.04$. (b) X-ray (006) rocking curve of the $x=0.04$ crystal, which shows a FWHM of only 0.1°. (c) Geometry of the contact pads on a ρ_c sample. (d) A ρ_c sample with lead wires attached.

The mixture of raw powders is well ground and calcined at 750 °C for 12 h, then at 920 °C for 12 h for four times in alumina crucibles, with regrinding between each calcination. After the last calcination and regrinding, the powders are isostatically pressed into a rod shape with typical dimensions of 7 mm$\phi \times$150 mm, and finally sintered at 1200 °C for 15 h in air to form the feed-rod. Calcination and regrinding for more than four times before the final sintering make the polycrystalline materials highly homogeneous, and this homogeneity is important for the sintered feed-rod to become dense and hard, which ensures the molten zone to be well stabilized during the TSFZ operation.

The solvent material, which is used to lower the temperature of the molten zone, is prepared to have the cation ratio of $La:Sr:Cu=(2-x):x:3$ for each x. We use 0.5 g of the solvent for the TSFZ growth. The TSFZ operation is carried out using an infrared image furnace (NEC Machinery SC K-15HD) with two halogen lamps and double ellipsoidal mirrors in the atmosphere of flowing dried air. To cut off reflections of the light from high angles, a quartz tube (which encloses the moving rods) is partly covered with aluminum foils to make a narrow window; this sharpens the temperature profile and helps to stabilize the molten zone.[33] Use of a seed crystal helps the whole rod to become a single crystal. The growth rate is kept constant at 1.0 mm/h (or less). A photograph of our TSFZ-grown crystal with $x=0.04$ is shown in Fig. 1(a) as an example, together with its x-ray rocking curve [Fig 1(b)]. The full width at half maximum (FWHM) of the (006) rocking curve shown in Fig. 1(b) is

only 0.1°, which is the smallest reported value for LSCO single crystals. (The x-ray beam is always wide enough to cover the whole specimen when the rocking curve is taken.)

After the growth is finished, the whole chunk of crystal is annealed at 850 °C for 20 h in air to remove thermal stresses formed during the floating zone growth. The crystallographic axes are precisely determined by the x-ray back-reflection Laue method, which also reveals that the typical growth direction is [110] (in the notation of high-temperature tetragonal phase). The samples for the present measurements are shaped into thin platelets with typical dimensions of $2.0 \times 0.5 \times 0.2$ mm^3, with the wide faces exactly parallel to the ab (ac) planes within an error of 1° for the in-plane (out-of-plane) measurements.

The samples with $x \leqslant 0.05$ are carefully annealed in pure Ar gas at 400 °C for 20 h to remove excess oxygen. It should be noted that in the lightly doped region the transport properties are strongly affected by the excess oxygen; even a slight amount of excess oxygen can easily cause phase-separated oxygen-rich regions which show superconductivity. (Many of the early data of lightly doped LSCO, like those of Ref. 34, were actually contaminated by the superconductivity caused by the excess oxygen.) We have examined various annealing conditions and found that annealing at higher temperature and/or for longer time in pure Ar does not change the resistivity any more; therefore, we have concluded that the above annealing is sufficient to dispose of the excess oxygen while minimizing the possible decomposition. On the other hand, samples with $x = 0.08$ and 0.10 are annealed at 800 °C for 40 hours in air, followed by rapid quenching to room temperature, to remove oxygen defects[35] that cause additional electron scattering in moderately-doped and overdoped samples.

B. Measurements

The in-plane and out-of-plane resistivities (ρ_{ab} and ρ_c) are measured using a standard ac four-probe method. Note that, since we can obtain samples that are long along the c axis, we do not need to use a complicated technique, such as the Montgomery method, for the ρ_c measurement in the case of LSCO. The contact pads are hand-drawn on polished sample surfaces with gold paint, followed by a heat treatment at 400 °C for 30 min in air, which makes the gold particles to well adhere to the crystal surface [the high-temperature annealing to remove excess oxygen (or oxygen defects) are done after this process]. For the current contacts, the whole area of two opposing side faces is painted with gold to ensure uniform current flow through the sample. After the annealing, thin gold wires are attached to the contact pads using silver epoxy, which electrically and mechanically binds the wire to the sample; the contact resistance with this technique is less than 1 Ω. The photographs in Figs. 1(c) and 1(d) show the geometry of the contacts and how the leads are attached.

The uncertainty in the absolute values of ρ_{ab} and ρ_c is minimized by using relatively long samples (at least 2 mm long) and by painting narrow contact pads with a width of 50–80 μm; total errors in the absolute values are less than 10%. We note that, although the measurements employ a simple four-probe method, each sample has four voltage contacts (two on each side face) and the resistivity is measured using both pairs [see Fig. 1(d)]. Sometimes the resistivity values from the two voltage pairs do not agree, which is an indication of some inhomogeneity (or microcrack) in the sample; we reject the data when such a discrepancy is observed, and all the data shown here are measured on samples for which the two data sets match within 5%. We also confirm that the resistivity data measured on different pieces of crystals from the same batch are reproducible within 10% as long as the samples are free from inhomogeneity.

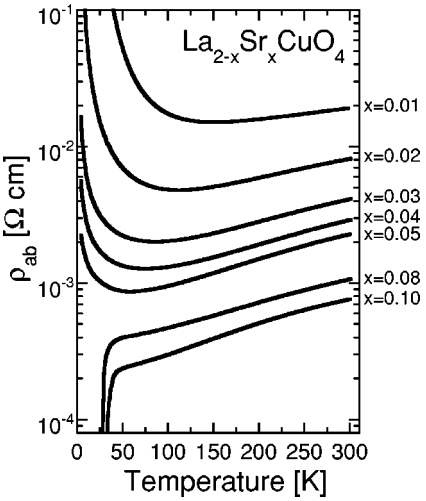

FIG. 2. Temperature dependences of ρ_{ab} of LSCO single crystals with $x = 0.01$–0.10.

III. RESULTS

Figure 2 shows the temperature dependences of ρ_{ab} of our crystals with the vertical axis in the logarithmic scale; this figure is essentially a partial reproduction of the data from Ref. 29, except for the $x = 0.10$ data that are new. The absolute value of ρ_{ab} is among the smallest ever reported[23,36] for each x. This fact, together with the very sharp x-ray rocking curve, indicates that the single crystals studied here are of very high quality. As emphasized in Ref. 29, the temperature dependence of ρ_{ab} is metallic ($d\rho_{ab}/dT > 0$) at moderate temperatures even in the samples where ρ_{ab} exceeds 2 mΩ cm, which corresponds to a $k_F l$ value[29] of less than 1, and thus the Mott-Ioffe-Regel limit for metallic transport is strongly violated; we have argued[29] that this behavior, in combination with mobility that is only weakly doping dependent, is best understood to result from a self-organized network of hole-rich regions that constitute the path for the charge transport.

Figure 3 shows the temperature dependence of ρ_c for the same doping range. In the $\rho_c(T)$ profile of LSCO, a clear kink is usually observed at the structural phase transition temperature from the high-temperature tetragonal phase to the low-temperature orthorhombic (LTO) phase;[2,22,24,28] for all the compositions of the present study, however, the structural phase transition occurs at temperatures higher than 300

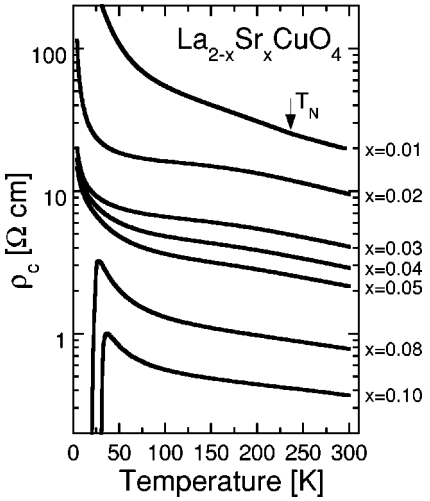

FIG. 3. Temperature dependences of ρ_c of LSCO single crystals with $x=0.01-0.10$. The arrow marks a kink at the Néel temperature for $x=0.01$.

K (Ref. 37), except for the $x=0.10$ sample which show a LTO transition at 293 K. We note that the data for $x=0.01$ show a kink at 240 K, which corresponds to the Néel temperature T_N and not to the LTO transition temperature. [A kink in the $\rho_c(T)$ curves at T_N has been reported[38,39] for antiferromagnetic YBCO, but not for LSCO before.] It is useful to note that, although ρ_c increases with decreasing temperature in all the samples, the temperature dependence of ρ_c is rather weak at moderate temperatures (for example, ρ_c of the $x=0.02$ sample shows only a factor of 2 increase from 300 to 50 K), and a negative curvature ($d^2\rho_c/dT^2<0$) is observed in the $\rho_c(T)$ profile for $x=0.02$ and 0.03 at temperatures above 100 K (which can be seen in Fig. 4). This negative curvature is in sharp contrast to the steeply positive curvature of $\rho_c(T)$ of Bi-2212 (Ref. 15) or Bi-2201 (Ref. 17) below the pseudogap temperature. At lower temperatures below 50 K, the $\rho_c(T)$ curves of all the samples show strongly diverging behaviors, which is in clear correspondence with the localization behavior in $\rho_{ab}(T)$ at low temperatures [except for the $x=0.08$ and 0.10 samples whose $\rho_{ab}(T)$ curves show an insulating behavior only when the superconductivity is suppressed by a high magnetic field[21]].

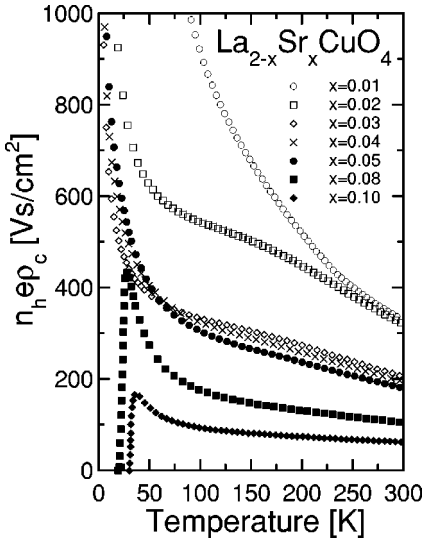

FIG. 4. Temperature dependences of $n_he\rho_c$, which corresponds to the inverse mobility of the doped holes along the c axis, for $x=0.01-0.10$.

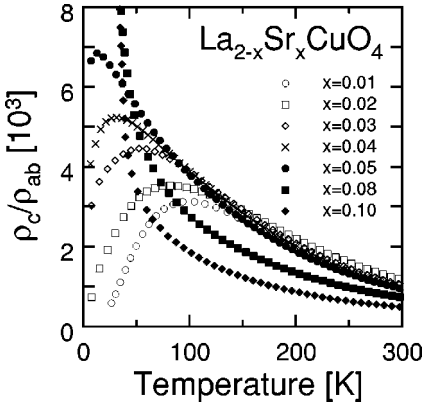

FIG. 5. Temperature dependences of the resistivity anisotropy ratio ρ_c/ρ_{ab} for $x=0.01-0.10$.

An intriguing aspect of the $\rho_c(T)$ data is that their profile does not change much with x [namely, the $\rho_c(T)$ data are almost parallel shifted for different x] at moderate temperatures, as is the case with the $\rho_{ab}(T)$ data. To examine the doping dependence of the $\rho_c(T)$ in detail, we plot the temperature dependences of $n_he\rho_c$, which corresponds to the inverse mobility μ_c^{-1} of the doped holes along the c axis, where e is the electronic charge and n_h is the nominal hole concentration given by $2x/V$ (the unit-cell volume V is $3.8\times3.8\times13.2$ Å^3), as we did for $\rho_{ab}(T)$ in Ref. 29. As shown in Fig. 4, the absolute magnitude of $n_he\rho_c$ at 300 K changes only by $\sim40\%$ in the nonsuperconducting regime (from $x=0.01$ to 0.05), although it starts to change quickly in the superconducting regime (above $x=0.05$). The weak x-dependence of $n_he\rho_c$ at 300 K in the nonsuperconducting regime is rather similar to the behavior of the inverse in-plane mobility μ_{ab}^{-1}, that also changes only by $\sim40\%$ from $x=0.01$ to 0.05 (Ref. 29).

The most surprising feature we find in this work is that ρ_c/ρ_{ab} at moderate temperatures is almost completely independent of doping in the nonsuperconducting regime ($0.01\leqslant x\leqslant0.05$), as illustrated in Fig. 5. When x exceeds 0.05 and enters the superconducting regime, ρ_c/ρ_{ab} starts to become smaller with increasing x. (The implication of this result is discussed in detail in Sec. IV.) Also, all the samples in Fig. 5 show strongly temperature-dependent ρ_c/ρ_{ab}, and in the nonsuperconducting samples ($x\leqslant0.05$) there is a peak that moves systematically to higher temperature with decreasing x. When one compares Fig. 5 to Fig. 2, it becomes clear that the peak temperature of the anisotropy corresponds to the onset of the insulating behavior in $\rho_{ab}(T)$; namely, the decrease of ρ_c/ρ_{ab} with decreasing temperature is determined by the rapid increase in ρ_{ab}. The occurrence of the peak in ρ_c/ρ_{ab} means that the strong localization of the carriers causes ρ_{ab} to diverge more rapidly than ρ_c, and as a result the system becomes less two dimensional in the strongly

localized state; this can be rephrased that the strong localization causes the system to become a ''three-dimensional'' insulator where the carriers cannot move in any direction.

It is worth noting that it is *not* the establishment of the long-range antiferromagnetic order but the strong localization effect that causes ρ_c/ρ_{ab} to decrease; in this regard, our result disagrees with the interpretation of Kitajima *et al.*[40] for the ρ_c/ρ_{ab} behavior of insulating $Bi_2Sr_2ErCu_2O_8$. Our sample with $x=0.01$ clearly shows that ρ_c/ρ_{ab} continues to increase with decreasing temperature (which means that the charge confinement becomes increasingly effective) even below the Néel temperature until the carriers start to localize.

IV. DISCUSSIONS

As seen in Fig. 3, the temperature dependence of ρ_c at moderate temperatures (100–300 K) is weak for $x \geqslant 0.02$, which is in contrast to the $\rho_c(T)$ behaviors of Bi-2212 or Bi-2201 where $\rho_c(T)$ shows a steep upturn below the pseudogap temperature [a steep upturn in $\rho_c(T)$ of LSCO is only observed at low temperature (below ~ 50 K), which is most likely associated with the strong localization]. Since the *c*-axis transport in any cuprate should necessarily reflect the *c*-axis matrix element that tends to amplify the development of the pseudogap with a $d_{x^2-y^2}$ symmetry, the $\rho_c(T)$ behavior of underdoped LSCO means either that the pseudogap is already fully developed at 300 K, or that the pseudogap has a symmetry different from $d_{x^2-y^2}$. (The photoemission experiment has observed a pseudogap in LSCO only in the angle-integrated mode, and the temperature evolution was not studied.[41]) Note also that the published ARPES results to date have reported[19] that the Fermi surface in the underdoped LSCO is observed only near the $(\pm\pi,0)$, $(0,\pm\pi)$ points (a one-dimensional-like Fermi surface), which is incompatible with the concept of the pseudogap with a $d_{x^2-y^2}$ symmetry; this fact might also be related to the weak temperature dependence of ρ_c at moderate temperatures. (It should be noted, however, that very recent ARPES measurements of the lightly doped LSCO succeeded in observing a developing band at the nodal points,[42] so the picture of the Fermi surface of LSCO is not yet finalized.) In any case, we expect that future ARPES measurements will help understanding the behavior of $\rho_c(T)$ in LSCO.

The most illuminating observation is that the resistivity anisotropy ρ_c/ρ_{ab} near room temperature is almost independent of x for $0.01 \leqslant x \leqslant 0.05$ (Fig. 5). In this x independent regime, the magnitude of ρ_c/ρ_{ab} is ~ 1000 at 300 K and increases with decreasing temperature, which indicates that the same charge confinement mechanism is at work down to $x=0.01$; interestingly, this range of x $(0.01-0.05)$ corresponds to the region where the neutron experiments have found diagonal spin stripes.[43–45] As already mentioned in Sec. III, the metallic in-plane transport that violates the Mott-Ioffe-Regel limit suggests[29] that the transport is occurring through a self-organized network of hole-rich regions[32] that constitute the path for the charge transport. The striking x independence of ρ_c/ρ_{ab} is naturally understood in this picture of transport through a self-organized network, because in such a case the transport anisotropy is determined by the local electronic nature of the hole-rich segment that is presumably unchanged with x (only the average in-plane distance between the hole-rich paths changes with x). Therefore, the behavior of ρ_c/ρ_{ab} in the lightly doped region is consistent with the self-organized-network picture, and gives strong support to it.

It should be noted that the *c*-axis mobility, as well as the ρ_c/ρ_{ab} ratio, quickly changes when x enters into the superconducting regime. As can be seen in Fig. 4, $n_h e \rho_c$ at 300 K changes by a factor of 3 from $x=0.05$ to 0.10, which indicates that the *c*-axis hopping quickly becomes easier as x is increased above 0.05. Correspondingly, the anisotropy ratio at moderate temperatures starts to show a decrease above $x=0.05$, which means that the charges are increasingly less confined in this doping range. This sharp change in the *c*-axis transport properties across $x=0.05$ is in contrast to the smooth change of the in-plane transport properties, where the mobility at 300 K changes very smoothly as $\sim\sqrt{x}$ (Ref. 29), neglecting the superconductor-to-insulator transition that occurs at low temperature. As discussed in Ref. 29, the fact that the in-plane mobility changes slowly and smoothly, and is governed by a simple function of x from $x=0.01$ to 0.17, strongly suggests that the mechanism of the in-plane charge transport is essentially unchanged from the antiferromagnetic regime to optimum doping; since the transport in the antiferromagnetic regime is likely to be governed by a self-organized network (which can be interpreted to be a generalized version of the ''stripes''[32]), the charge transport in the whole phase diagram up to optimum doping appears to be governed by such an electron self-organization, which also gives a natural picture for the charge confinement. The difference in the x dependence between μ_c and μ_{ab} probably indicates that the *c*-axis coupling (or correlation) between the two-dimensional networks is more susceptible to the change in x than the properties of the network itself. It is intriguing to note that the emergence and increase of T_c appear to be related to an increase in the *c*-axis coupling between the self-organized network.

V. SUMMARY

The *ab*- and *c*-axis resistivities are measured in the lightly to moderately doped LSCO single crystals, and the resistivity anisotropy is analyzed to sort out the transport mechanism of this prototype cuprate. At moderate temperatures, the temperature dependence of ρ_c in the underdoped LSCO is much weaker than that of underdoped Bi-2212 or Bi-2201; we discuss that this difference in the $\rho_c(T)$ behavior is related to the differences in both the Fermi-surface topology and to the way in which the pseudogap develops on the Fermi surface. Moreover, we found that ρ_c/ρ_{ab} near room temperature is almost completely independent of doping for $0.01 \leqslant x \leqslant 0.05$. This result supports the picture that the holes form a self-organized network of hole-rich path, which was originally suggested[29] from the unusually metallic in-plane transport of the holes in the lightly doped region; in this picture, it is understood that the bandlike in-plane transport takes place through the self-organized network, while the *c*-axis transport is essentially an incoherent hopping between the net-

works, in which the strength of the confinement does not change with x in the lightly doped region. Our data for $x > 0.05$ suggest that the weakening of the c-axis charge confinement is related to the emergence of the superconductivity, while the in-plane transport mechanism appears to be unchanged from $x = 0.01$ to optimum doping.

ACKNOWLEDGMENTS

We thank A. Fujimori and S. A. Kivelson for helpful discussions, and T. Sasagawa and K. Kishio for valuable suggestions for the crystal growth. X.F.S. acknowledges support from JISTEC.

*Email address: komiya@criepi.denken.or.jp
†Email address: ando@criepi.denken.or.jp

[1] P.W. Anderson, Science **256**, 1526 (1992).
[2] Y. Nakamura and S. Uchida, Phys. Rev. B **47**, 8369 (1993).
[3] K. Takenaka, K. Mizuhashi, H. Takagi, and S. Uchida, Phys. Rev. B **50**, 6534 (1994).
[4] Y. Ando, G.S. Boebinger, A. Passner, N.L. Wang, C. Geibel, and F. Steglich, Phys. Rev. Lett. **77**, 2065 (1996).
[5] For a review, see S.L. Cooper and K.E. Gray, in *Physical Properties of High Temperature Superconductors IV*, edited by D.M. Ginsberg (World Scientific, Singapore, 1994).
[6] W.E. Pickett, Rev. Mod. Phys. **61**, 433 (1989).
[7] A.G. Rojo and K. Levin, Phys. Rev. B **48**, 16861 (1993).
[8] N. Kumar and A.M. Jayannavar, Phys. Rev. B **45**, 5001 (1992).
[9] M.J. Graf, D. Rainer, and J.A. Sauls, Phys. Rev. B **47**, 12089 (1993).
[10] L.B. Ioffe and A.J. Millis, Phys. Rev. B **58**, 11631 (1998).
[11] M. Suzuki and T. Watanabe, Phys. Rev. Lett. **85**, 4787 (1999).
[12] V.M. Krasnov, A. Yurgens, D. Winkler, P. Delsing, and T. Claeson, Phys. Rev. Lett. **84**, 5860 (2000).
[13] T. Xiang and J.M. Wheatley, Phys. Rev. Lett. **77**, 4632 (1996).
[14] M.R. Norman, H. Ding, M. Randeria, J.C. Campuzano, T. Yokoya, T. Takeuchi, T. Takahashi, T. Mochiku, K. Kadowaki, P. Guptasarma, and D.G. Hinks, Nature (London) **392**, 157 (1998).
[15] T. Watanabe, T. Fujii, and A. Matsuda, Phys. Rev. Lett. **79**, 2113 (1997).
[16] T. Watanabe, T. Fujii, and A. Matsuda, Phys. Rev. Lett. **84**, 5848 (2000).
[17] A.N. Lavrov, Y. Ando, and S. Ono, Europhys. Lett. **57**, 267 (2002).
[18] X.J. Zhou, P.V. Bogdanov, S.A. Kellar, T. Noda, H. Eisaki, S. Uchida, Z. Hussain, and Z.-X. Shen, Science **286**, 268 (1999).
[19] A. Ino, C. Kim, M. Nakamura, T. Yoshida, T. Mizokawa, Z.-X. Shen, A. Fujimori, T. Kakeshita, H. Eisaki, and S. Uchida, Phys. Rev. B **62**, 4137 (2000).
[20] T. Ito, H. Takagi, S. Ishibashi, T. Ido, and S. Uchida, Nature (London) **350**, 596 (1991).
[21] Y. Ando, G.S. Boebinger, A. Passner, T. Kimura, and K. Kishio, Phys. Rev. Lett. **75**, 4662 (1995).
[22] F. Nakamura, M. Kodama, S. Sakita, Y. Maeno, T. Fujita, H. Takahashi, and N. Môri, Phys. Rev. B **54**, 10 061 (1996).
[23] T. Kimura, S. Miyasaka, H. Takagi, K. Tamasaku, H. Eisaki, S. Uchida, K. Kitazawa, M. Hiroi, M. Sera, and N. Kobayashi, Phys. Rev. B **53**, 8733 (1996).
[24] N.E. Hussey, J.R. Cooper, Y. Kodama, and Y. Nishihara, Phys. Rev. B **58**, R611 (1998).
[25] T. Shibauchi, H. Kitano, K. Uchinokura, A. Maeda, T. Kimura, and K. Kishio, Phys. Rev. Lett. **72**, 2263 (1994).
[26] S. Uchida, K. Tamasaku, and S. Tajima, Phys. Rev. B **53**, 14 558 (1996).
[27] S.V. Dordevic, E.J. Singley, D.N. Basov, S. Komiya, Y. Ando, E. Bucher, C.C. Homes, and M. Strongin, Phys. Rev. B **65**, 134511 (2002).
[28] G.S. Boebinger, Y. Ando, A. Passner, T. Kimura, M. Okuya, J. Shimoyama, K. Kishio, K. Tamasaku, N. Ichikawa, and S. Uchida, Phys. Rev. Lett. **77**, 5417 (1996).
[29] Y. Ando, A.N. Lavrov, S. Komiya, K. Segawa, and X.F. Sun, Phys. Rev. Lett. **87**, 017001 (2001).
[30] T. Thio, C.Y. Chen, B.S. Freer, D.R. Gabbe, H.P. Jenssen, M.A. Kastner, P.J. Picone, N.W. Preyer, and R.J. Birgeneau, Phys. Rev. B **41**, 231 (1990).
[31] S.W. Cheong, M.F. Hundley, J.D. Thompson, and Z. Fisk, Phys. Rev. B **39**, 6567 (1989).
[32] S.A. Kivelson, E. Fradkin, and V.J. Emery, Nature (London) **393**, 550 (1998).
[33] C.-H. Lee, N. Kaneko, S. Hosoya, K. Kurahashi, S. Wakimoto, K. Yamada, and Y. Endoh, Supercond. Sci. Technol. **11**, 891 (1998).
[34] H. Takagi, T. Ido, S. Ishibashi, M. Uota, S. Uchida, and Y. Tokura, Phys. Rev. B **40**, 2254 (1989).
[35] H. Kanai, J. Mizusaki, H. Tagawa, S. Hoshiyama, K. Hirano, K. Fujita, M. Tezuka, and T. Hashimoto, J. Solid State Chem. **131**, 150 (1997).
[36] T. Sasagawa, Y. Togawa, J. Shimoyama, A. Kapitulnik, K. Kitazawa, and K. Kishio, Phys. Rev. B **61**, 1610 (2000).
[37] M.A. Kastner, R.J. Birgeneau, G. Shirane, and Y. Endoh, Rev. Mod. Phys. **70**, 897 (1998).
[38] A.N. Lavrov, M.Yu. Kameneva, and L.P. Kozeeva, Phys. Rev. Lett. **81**, 5636 (1998).
[39] A.N. Lavrov, Y. Ando, K. Segawa, and J. Takeya, Phys. Rev. Lett. **83**, 1419 (1999).
[40] T. Kitajima, T. Takayanagi, T. Takemura, and I. Terasaki, J. Phys.: Condens. Matter **11**, 3169 (1999).
[41] A. Ino, T. Mizokawa, K. Kobayashi, A. Fujimori, T. Sasagawa, T. Kimura, K. Kishio, K. Tamasaku, H. Eisaki, and S. Uchida, Phys. Rev. Lett. **81**, 2124 (1998).
[42] A. Fujimori and Z.-X. Shen, (private communication).
[43] S. Wakimoto, R.J. Birgeneau, M.A. Kastner, Y.S. Lee, R. Erwin, P.M. Gehring, S.H. Lee, M. Fujita, K. Yamada, Y. Endoh, K. Hirota, and G. Shirane, Phys. Rev. B **61**, 3699 (2000).
[44] M. Matsuda, M. Fujita, K. Yamada, R.J. Birgeneau, M.A. Kastner, H. Hiraka, Y. Endoh, S. Wakimoto, and G. Shirane Phys. Rev. B **62**, 9148 (2000).
[45] M. Matsuda, M. Fujita, K. Yamada, R.J. Birgeneau, Y. Endoh, and G. Shirane, Phys. Rev. B **65**, 134515 (2002).